Analyzing Performance of Eigenvalue-based Spectrum Sensing within LoRaCog Framework

Batool Jaafar Bashar and Hikmat Abdullah

Al-Nahrain University, Baghdad, Iraq

https://doi.org/10.26636/jtit.2026.2.2576

Abstract — The CR technology enhances spectrum utilization by allowing access to unused licensed channels, while spectrum sensing allows secondary users to verify channel availability before the transmission. This study relies on the LoRaCog framework, a solution integrating the CR technology with LoRa LPWAN networks, to evaluate the performance of eigenvalue-based detection algorithms, such as maximum eigenvalue detection (MED), maximum to minimum eigenvalue (MME), energy-to-minimum eigenvalue (EME) and maximum-to-mean eigenvalue detection (MMED), with the comparisons based on energy detection (ED). The said algorithms were evaluated under three scenarios characterized by an increasing degree of complexity. These included the following: an ideal additive white Gaussian noise (AWGN) channel, followed by a multipath fading channel with noise uncertainty using a SISO receiver and, finally, a SIMO multiantenna receiver system. The simulation results for the AWGN channel showed that the ED algorithm achieved the best detection probability and the lowest sensing time. When multipath fading and noise uncertainty were introduced, eigenvalue-based algorithms achieved higher detection probabilities while maintaining comparable detection times. The MME algorithm achieved the highest detection probability when used with the SIMO multiantenna reception system.

Keywords — CR, eigenvalue-based detection, LoRa networks, LPWAN, spectrum sensing

1. Introduction

Many solutions have been proposed to address the challenges arising from inefficient spectrum management, among which the CR technology has emerged as a promising approach [1]. CR enables dynamic spectrum access by allowing secondary users (SUs) to opportunistically utilize frequency bands when primary users (PUs) are inactive, ensuring also that no interference is caused to licensed users [2], [3]. Spectrum sensing plays a crucial role in this mechanism by enabling SUs to determine whether a given frequency band is occupied before initiating transmission [4], [5].

Low-power wide-area networks (LPWANs) are among the primary wireless technologies that support applications of the Internet of Things (IoT). Among these, LoRa networks are distinguished by their ability to provide long-range communication while maintaining low power consumption. LoRa networks typically operate in unlicensed frequency bands. However, these bands have become increasingly congested due to the rapid growth in the popularity of IoT devices. Such congestion may lead to increased packet collisions and reduced communication reliability, particularly in dense deployment environments [6], [7].

Several studies have investigated integrating CR into LoRa networks using a cognitive LoRa framework (LoRaCog). In this framework, LoRa gateways are equipped with spectrum sensing capabilities, allowing them to monitor licensed channels and opportunistically access temporarily unused spectrum while preserving the existing LoRa infrastructure [8]. However, achieving reliable spectrum sensing in such environments remains a major challenge, particularly under low signal-to-noise ratio (SNR) conditions.

Because of its simplicity, energy detection (ED) is one of the most widely used spectrum-sensing techniques. However, its performance deteriorates significantly in low-SNR environments due to the SNR wall effect. To overcome these limitations, eigenvalue-based spectrum sensing algorithms have attracted considerable attention. These methods rely on the statistical properties of the covariance matrix of the received signal, allowing the detection of a primary user without prior knowledge of the signal structure or the noise power [2], [9], [10].

This study evaluates the performance of several eigenvalue-based spectrum sensing algorithms within the LoRaCog framework. The algorithms investigated include maximum eigenvalue detection (MED), maximum-to-minimum eigenvalue (MME), energy-to-minimum eigenvalue (EME), and maximum-to-mean eigenvalue detection (MMED). Performance of these algorithms is analyzed in terms of detection capability and sensing time. Furthermore, these algorithms are compared with the conventional ED technique under different channel conditions, including the ideal AWGN channel, multipath fading channels with noise uncertainty, and a SIMO multi-antenna reception system.

2. Literature Survey

Many studies have focused on improving spectrum utilization and scalability in LoRa and LPWAN networks operating in dense IoT environments. The authors of [11] discussed the

limitations of LoRaWAN networks, particularly spectrum congestion and scalability challenges within industrial, scientific, and medical (ISM) bands. The study highlighted the need for more flexible and efficient spectrum management approaches. In this context, in [8], the LoRaCog framework is introduced, integrating CR capabilities into LoRa networks by assigning spectrum sensing tasks to gateway nodes. This framework enables the dynamic utilization of licensed channels while preserving the existing LoRa infrastructure. Furthermore, in [12], the integration of CR technologies with LPWAN systems is reviewed and the main challenges related to spectrum sensing reliability, interference management, and energy efficiency in IoT environments are discussed.

The authors of [13] reviewed several aspects of the ED algorithm in CR networks and noted that it remains one of the most commonly adopted sensing techniques due to its ease of implementation. However, previous studies have shown that the effectiveness of this technique deteriorates significantly under low SNR conditions and in the presence of noise uncertainty. These limitations lead to reduced detection reliability and to the SNR wall effect [13], [14].

To address these limitations, many studies have focused on developing spectrum-sensing algorithms based on the eigenvalues of the received signal's covariance matrix. Paper [10] established the theoretical foundation for these techniques by demonstrating that the presence of a PU signal changes the eigenvalue distribution of the covariance matrix of the received signal. This property enables signal detection without requiring prior knowledge of the signal structure or noise power. Subsequently, several studies attempted to improve the reliability of eigenvalue-based sensing algorithms under different wireless channel conditions. For example, in [15], the development of eigenvalue-based sensing techniques is reviewed and the article reports that these methods provide greater reliability than conventional sensing approaches, particularly under noise uncertainty conditions.

More recent studies have further demonstrated the effectiveness of eigenvalue-based techniques in fading environments, where improved detection performance can be achieved at low SNR levels compared to conventional ED methods [16].

Recent works focus mainly on developing individual sensing algorithms or integrating spectrum sensing techniques with machine learning in conventional wireless communication environments. The number of studies covering multiple eigenvalue-based sensing algorithms in cognitive LoRa networks under realistic wireless channel conditions remains relatively limited.

3. Overview of the LoRa Cognitive Framework

This section provides an overview of the LoRa cognitive framework (LoRaCog) introduced in [8] – a solution integrating CR concepts into LoRa networks and enabling gateways to perform sensing to improve spectrum efficiency. The LoRaCog framework extends the traditional LoRaWAN architecture by enabling gateways to access licensed channels when they are temporarily unused by PUs. This extension aims to improve spectrum efficiency and mitigate spectrum congestion.

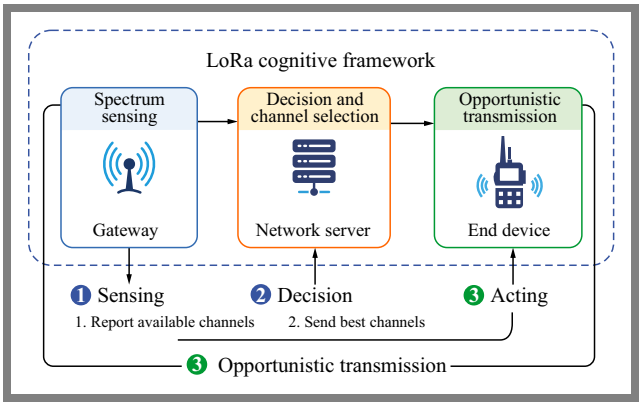

Fig. 1. Operational workflow of the LoRaCog framework.

The framework maintains the LoRaWAN network infrastructure, consisting of end devices (EDs), gateways (GWs) and the (NS). However, cognitive functions are integrated into this architecture by assigning spectrum sensing and decision-making tasks to specific components within the network, such as gateways, in order to optimize spectrum usage and improve overall network performance.

As shown in Fig. 1, the LoRaCog principle comprises three stages. First, spectrum sensing is performed at the gateway level, where the gateways monitor licensed channels and collect signal samples to detect the presence of a PU. Due to the availability of a stable power source, elevated deployment sites, and higher processing capabilities, gateways are suitable for implementing sensing algorithms. Then, the sensing results are sent to the NS, where the decision is made. Based on sensing reports from one or more gateways, the NS selects the channel, determines whether it is available for opportunistic access, and chooses the most suitable channel for transmission. Finally, the terminal devices that operate as SUs and benefit from gateway sensing transmit data based on NS information. These devices do not participate in the spectrum-sensing process due to their limited computational capabilities and strict energy consumption constraints. Instead, they rely entirely on the decisions before the uplink transmission begins.

4. System Model

At the beginning of the sensing process, a specific number of baseband samples of the received signal is collected. Let $x(n)$ represent the received sample in discrete time. The spectral sensing task can be formulated as a binary hypothesis test to determine whether the PU signal is present or absent in the observed frequency range [5].

$$H_0 : x(n) = n(n) \,, \tag{1}$$

$$H_1 : x(n) = s(n) + n(n) \,, \tag{2}$$

where $s(n)$ denotes the PU signal and $n(n)$ represents the additive noise component.

Noise is typically modelled as additive white Gaussian noise (AWGN) with zero mean and variance σ^2:

$$n(n) \sim CN\left(0, \sigma^2\right) . \tag{3}$$

In real wireless environments, the exact noise power may deviate from its nominal value due to hardware imperfections and environmental variations. This phenomenon is commonly referred to as noise uncertainty, which can be modeled as [2]:

$$\sigma_{eff}^2 = \sigma^2\left(1+\delta\right) , \tag{4}$$

where δ represents the uncertainty factor.

Because wireless channels often experience multipath fading, the received signal may contain several delayed replicas of the transmitted signal. The received signal can therefore be expressed in the following form:

$$x(n) = \sum_{k=0}^{L_h-1} h(k)\, s(n-k) + \eta(n) , \tag{5}$$

where $h(k)$ denotes the channel coefficient of the k-th propagation path and L_h represents the number of channel taps.

When multiple observation branches are considered, the received samples can be arranged in a vector form as follows.

$$x(n) = \left[x_1(n), x_2(n), \ldots, x_M(n)\right]^T . \tag{6}$$

To use the statistical properties of the received signal, the sample covariance matrix is estimated from the received samples:

$$R_x = \frac{1}{N}\sum_{n=1}^{N} x(n)\, x^H(n) . \tag{7}$$

Under the signal-present hypothesis, the covariance matrix can be expressed as:

$$R_x = R_s + \sigma^2 I , \tag{8}$$

where R_s denotes the covariance matrix of the signal component and I is the identity matrix.

The presence of the signal modifies the eigenvalue distribution of the covariance matrix, which forms the fundamental principle exploited by eigenvalue-based spectrum sensing algorithms [10].

5. Spectrum Sensing Algorithms

In this section, a summary of algorithms based on the eigenvalues of the covariance matrix is presented. The methods studied include maximum eigenvalue detection (MED), maximum–minimum eigenvalue detection (MME), energy with minimum eigenvalue (EME) and maximum-to-mean eigenvalue detection (MMED).

In the MED detector, the largest eigenvalue of the covariance matrix is used as the test statistic. Let the ordered eigenvalues of the covariance matrix be as follows:

$$\lambda_1 \geqslant \lambda_2 \geqslant \cdots \geqslant \lambda_M . \tag{9}$$

The MED test statistic is defined as:

$$T_{\mathrm{MED}} = \lambda_1 . \tag{10}$$

The MED algorithm is among the simplest eigenvalue-based algorithms. It only requires calculating the largest eigenvalue and since it relies on a single eigenvalue, it is more prone to deterioration in its detection capability, especially at the SNR level [9].

The MME detector uses the ratio between the largest and smallest eigenvalues of the covariance matrix:

$$T_{\mathrm{MME}} = \frac{\lambda_1}{\lambda_M} . \tag{11}$$

Estimating multiple eigenvalues increases computational complexity and sensing time compared to simpler detectors [15].

The EME detector combines energy detection with eigenvalue normalization. The received signal energy is first computed as:

$$E = \frac{1}{N}\sum_{n=1}^{N} \left|x(n)\right|^2 . \tag{12}$$

The test statistic is then defined as:

$$T_{\mathrm{EME}} = \frac{E}{\lambda_M} . \tag{13}$$

Normalization improves the detector's robustness against noise uncertainties compared to conventional ED methods. However, the requirement of calculating eigenvalues increases the computational cost [15].

The MMED evaluates the ratio of the largest eigenvalue to the average eigenvalue of the sample covariance matrix. The test statistic is defined as:

$$T_{MMED} = \frac{\lambda_{max}}{\frac{1}{M}\sum\limits_{i=1}^{M}\lambda_i} , \tag{14}$$

where $\lambda_{\max}$ denotes the largest eigenvalue and λ_i represents the eigenvalues of the covariance matrix.

Under the noise-only hypothesis, the eigenvalues tend to be close to each other, whereas the presence of a signal increases the dominant eigenvalue relative to the average eigenvalue. Similar to other detectors based on eigenvalues, this method requires covariance matrix estimation followed by eigenvalue decomposition [15].

5.1. Complexity Analysis of Spectrum Sensing Algorithms

The computational complexity of the spectrum sensing algorithms depends mainly on the operations required for signal processing and statistical analysis. ED requires only energy computation on the received signal samples, resulting in a relatively low computational complexity of $O(N)$, where N represents the number of received samples [13]. In contrast, eigenvalue-based sensing algorithms require covariance matrix estimation followed by eigenvalue decomposition. Since the decomposition of an $M \times M$ covariance matrix typically requires $O(M^3)$ operations, the computational cost of MED, MME, EME, and MMED is mainly dominated by this process [10].

However, these algorithms provide improved sensing reliability under low SNR and noise uncertainty conditions, representing a trade-off between computational complexity and sensing performance [15].

6. Eigenvalue-based Spectrum Sensing

Three scenarios of variable difficulty were adopted to test the efficiency of eigenvalue-based spectral sensing algorithms. The first scenario assumes an ideal AWGN channel and a SISO wireless communication system. The second scenario considers multipath fading and noise power uncertainty while maintaining a SISO system, while the third scenario is a modification of the second one, using a SIMO wireless communication system to improve detection reliability and benefit from spatial diversity.

A numerical simulation framework based on the LoRaCog architecture was used, in which spectral sensing is performed at the gateway level rather than at the terminal nodes, according to the centralized architecture, thereby reducing power consumption in low power IoT devices. The gateway collects baseband signal samples from the surrounding wireless environment during each sensing period. After receiving the signal and completing the sample collection, the covariance matrix of the received signal is developed. This matrix represents the fundamental statistical structure on which the eigenvalue-based sensing algorithms are based.

Subsequently, eigenvalue analysis was performed, where the resulting values were arranged in descending order. Spectral sensing algorithms rely on these values to extract the statistical properties. When there is a signal from the PU, the largest eigenvalue increases significantly, while the remaining eigenvalues often reflect background noise due to statistical correlations induced by the organized signal across the received samples.

The traditional ED statistic in the system model is also computed and serves as a primary reference for comparison with eigenvalue-based algorithms.

In the next part, the detection threshold was determined to ensure the accuracy of the spectral sensing process. In this study, the threshold was not calculated from a theoretical distribution, but was estimated numerically from the empirical distribution of the test statistic under the null hypothesis of noise only. Noise samples were generated, and the test statistic was calculated for each algorithm. Then, the detection threshold was chosen based on the desired false alarm probability.

The threshold was derived using the inverse cumulative distribution function of the test statistic under the noise-only hypothesis, and it can be expressed as follows:

$$\gamma = F_T^{-1}\left(1 - P_f\right), \tag{15}$$

where F_T^{-1} refers to the inverse cumulative distribution function of the test statistic, and P_f represents the desired false alarm probability.

Tab. 1. Simulation parameters.

Parameter	Symbol	Value
Number of samples	N	1024
SNR range	SNR	$(-20:1:5)$ dB
Noise variance	σ^2	1
Noise uncertainty factor	δ	0.2
Covariance matrix size	M	50
Multipath channel taps	L_h	3 (SISO), 4 (SIMO)
Monte Carlo realizations	MC	1000
ROC realizations	MCROC	3000
Sampling frequency	F_s	1 MHz
Signal bandwidth	B	200 kHz

After determining the threshold, the process of testing the algorithms began under the assumption of the presence of both signal and noise at different SNR values to simulate the PU signal in the wireless channel. The detection probability was then calculated by comparing the test statistic with the corresponding threshold.

Performance evaluation relied on two types of analysis. The first focuses on studying the detection probability as the SNR varies to evaluate the performance under low SNR conditions, while the second uses receiver operating characteristic (ROC) curves to show the relationship between detection and false alarm probabilities at different threshold values.

In addition to evaluating the performance of the sensing algorithms, the execution time of each algorithm was measured. In the LoRaCog framework, since spectral detection is performed at the gateway level, processing time directly affects the detection delay of the system. Therefore, the average execution time extracted from the simulation reflects the computational complexity.

7. Simulation Results

The simulation environment was implemented using Matlab and, in all scenarios, the number of samples received was fixed at $N = 1024$, while the covariance matrix size was set to $M = 50$.

The simulation generated baseband signals and then passed them through a low-pass FIR filter with a sampling frequency of $F_s = 1$ MHz and a bandwidth of $B = 200$ kHz. This configuration was adopted to simulate narrowband wireless signals commonly used in low-power IoT applications. The performance of the sensing algorithms was evaluated in an SNR range of –20 dB to 5 dB with a step size of 1 dB. In multipath environments, the wireless channel was modeled with $L_h = 3$ propagation paths for the SISO system and $L_h = 4$ for the SIMO system. The SIMO scenario used $N_r = 3$ receiving antennas. The effect of noise uncertainty was incorporated using a noise uncertainty factor of $\delta = 0.2$.

The detection thresholds were numerically estimated using the empirical cumulative distribution function under the noise-only hypothesis with a target false alarm probability of $P_f = 0.1$. Monte Carlo simulation with 1000 iterations was used

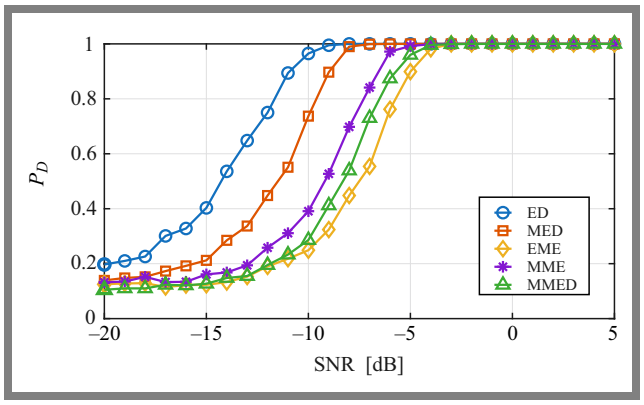

Fig. 2. Probability of detection versus SNR for spectrum detection algorithms under AWGN channel conditions.

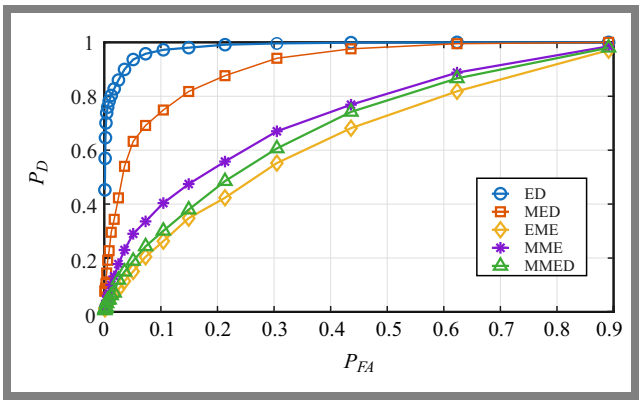

Fig. 3. ROC curves of P_D versus P_{FA} under AWGN channel conditions.

to analyze the probability of detection, while 3000 iterations were employed for ROC curve analysis.

Table 1 summarizes the simulation parameters used in this study.

The first scenario represents the ideal reference case, in which the received signal is affected only by AWGN with accurate knowledge of the noise power while employing the SISO receiver system. Figure 2 illustrates the relationship between the probability of detection of P_D and SNR, demonstrating the performance of the investigated spectrum detection algorithms under ideal channel conditions.

As the SNR increases, all evaluated algorithms exhibit gradual improvements in detection performance. However, the rate of improvement differs among the sensing techniques. The results indicate that ED achieves the highest sensing performance across most SNR ranges.

For instance, at SNR = –12 dB, ED achieves a detection probability of $P_D \approx 0.75$, whereas MED achieves 0.42. In contrast, the remaining eigenvalue-based techniques achieve detection probabilities below 0.20.

AWGN conditions with accurate noise power estimation, the statistical distinction between signal and noise becomes more evident, making the received signal energy a reliable indicator for signal detection and thereby improving sensing performance. Although MED performs worse than ED under AWGN conditions, its detection capability is influenced by the dominant eigenvalue of the covariance matrix, which becomes more pronounced in the presence of signal components.

At higher SNR levels, the performance gap between the evaluated techniques gradually decreases. At approximately SNR= –6 dB, all algorithms approach near-ideal sensing performance, where the probability of detection P_D approaches unity. This occurs because signal energy significantly exceeds the background noise energy, making signal detection easier regardless of the sensing technique employed.

To further analyze the sensing behavior under low SNR conditions, ROC curves were analyzed at SNR= –10 dB (Fig. 3).

The results obtained indicate that ED achieves superior sensing performance compared to eigenvalue-based techniques. At a false alarm probability of $P_{FA} = 0.05$, ED achieves

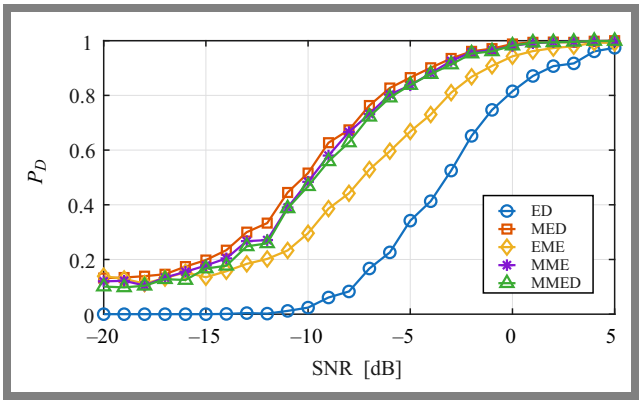

Fig. 4. Probability of detection versus SNR with multipath fading with uncertainty of noise.

$P_D \approx 0.92$, while MED and MME achieve 0.54 and 0.25, respectively. These observations further confirm the robustness of ED under ideal channel conditions and demonstrate its ability to achieve high detection performance while maintaining a low false alarm rate.

In the second scenario, more realistic operating conditions were considered by incorporating multipath fading effects and noise uncertainty while employing a SISO receiver system. Figure 4 illustrates the relationship between SNR and the probability of detection under these operating conditions.

The results show a noticeable degradation in the performance of the conventional ED technique. For example, at SNR = –10 dB, the detection probability decreases to $P_D \approx 0.021$, indicating a reduction in the sensing capability. This behavior can be attributed to the strong dependence of ED on accurate noise power estimation, where fluctuations in noise power increase the similarity between the two detection hypotheses, making the distinction between signal presence and signal absence more difficult.

At SNR = –10 dB, the obtained detection probabilities are: $P_D = 0.50$ (MED), $P_D = 0.4565$ (MME), $P_D = 0.4707$ (MMED) and $P_D = 0.2742$ (EME).

The eigenvalue-based sensing techniques maintain higher detection reliability under realistic channel conditions. MED benefits from the presence of dominant eigenvalues associated with signal components, whereas MME and MMED exploit eigenvalue ratios to enhance the separation between signal and

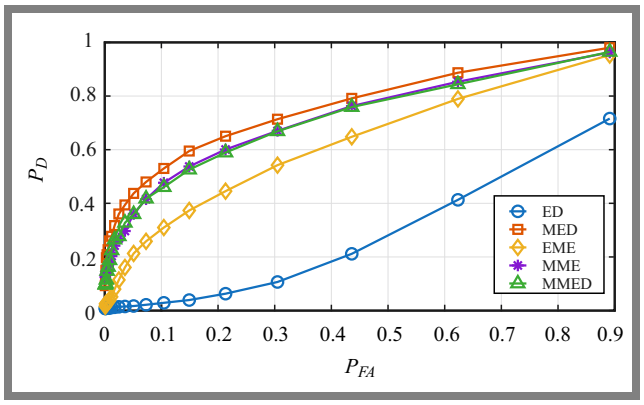

Fig. 5. ROC curves of P_D versus P_{FA} under multipath fading with noise uncertainty.

noise subspaces. EME also benefits from signal normalization using eigenvalues. However, its performance remains lower than that of the other techniques because of its sensitivity to variations associated with the minimum eigenvalue. The ROC curves for this case are presented in Fig. 5.

The ROC results further illustrate the behavior of the investigated sensing techniques under multipath fading and noise uncertainty conditions. At a false alarm probability of $P_{FA} = 0.1$, MED achieves a detection probability of $P_D \approx 0.68$, whereas ED remains below 0.05. The ROC curves of the eigenvalue-based techniques exhibit a steeper increase than those of ED, indicating a higher sensitivity to the presence of the primary user signal under realistic operating conditions. These observations indicate that eigenvalue-based sensing techniques preserve more reliable detection performance under realistic channel conditions and are less sensitive to noise power fluctuations than direct energy measurements.

The third scenario extends the previous environment by introducing spatial diversity through a SIMO receiver system with $N_r = 3$ receiving antennas while maintaining the same multipath fading conditions and noise uncertainty. Figure 6 illustrates the relationship between the probability of P_D detection and SNR for the sensing techniques investigated under spatial diversity conditions.

The results obtained indicate that all sensing techniques improve the detection performance compared to the previous SISO scenario. However, the improvement is more pronounced for eigenvalue-based sensing techniques. At SNR = –10 dB, the $P_D = 0.8045$ (MME), $P_D = 0.7813$ (MMED), $P_D = 0.6802$ (MED), and $P_D = 0.4972$ (EME).

In contrast, ED exhibits substantially lower performance under the same operating conditions, as spatial diversity provides a significant improvement in sensing reliability, particularly for eigenvalue-based sensing techniques. MED benefits from stronger dominant eigenvalues generated by multiple received observations, whereas MME and MMED use eigenvalue ratios more effectively as a result of the increased separation between signal and noise subspaces.

EME also benefits from the additional signal information provided by multiple antenna branches. However, its performance remains lower because of its sensitivity to variations associated with the minimum eigenvalue.

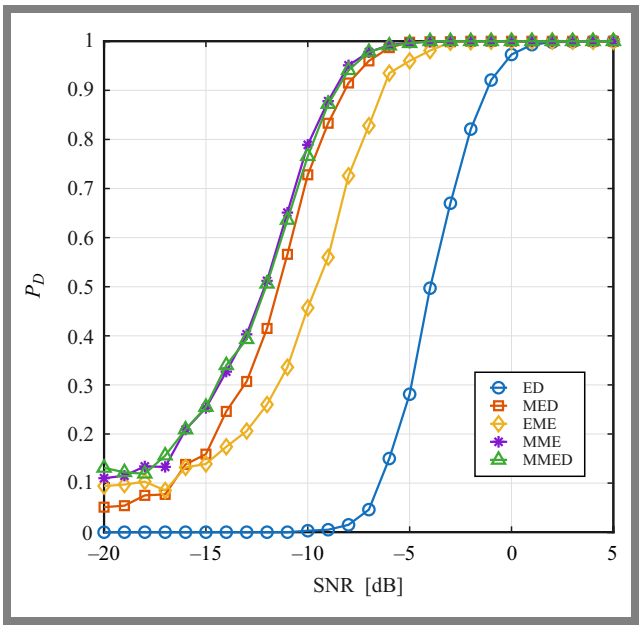

Fig. 6. Probability of detection versus SNR under the SIMO receiver system with multipath fading and noise uncertainty.

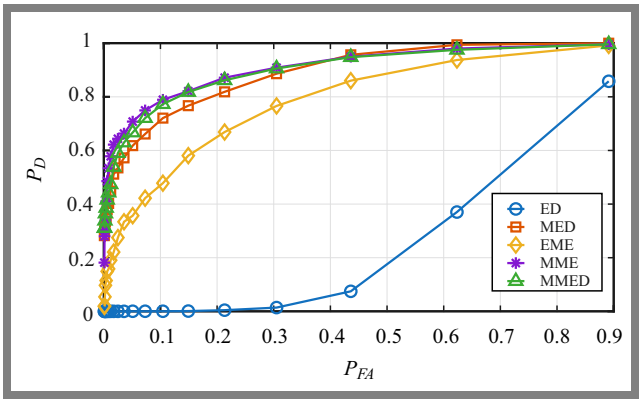

Fig. 7. ROC curves (P_D versus P_{FA}) under the SIMO receiver system with multipath fading and noise uncertainty.

The ROC curves obtained under SIMO operating conditions at SNR = –10 dB are presented in Fig. 7.

One may notice the superiority of MME under SIMO operating conditions. At a false alarm probability of $P_{FA} = 0.1$, both MME and MMED achieve detection probabilities exceeding 0.75, while MED achieves approximately 0.68. Furthermore, the ROC curves of MME and MMED exhibit steeper growth characteristics than those of the other techniques, showing a better sensitivity to the presence of the PU signal. These observations further confirm that spatial diversity improves the statistical separation between signal and noise components, thus enhancing sensing reliability.

The sensing time of the investigated spectrum-sensing techniques was also evaluated to analyze their computational requirements. The reported sensing time represents the total duration of the process, including both the observation interval required to collect the received samples and the time required to calculate the detection statistic.

The energy detection technique achieved the lowest sensing time of 1.084 ms. This low-sensing delay is primarily attributed to its simple implementation, as it relies only on direct energy calculations without additional processing. In contrast, eigenvalue-based sensing techniques require covariance matrix estimation and eigenvalue decomposition, resulting in higher computational costs and longer sensing times.

The average detection time of the eigenvalue-based techniques was 2.655 ms. EME, MME, and MMED exhibit similar sensing times, since they share the same fundamental computational stages which constitute the dominant computational burden in eigenvalue-based sensing techniques.

Although eigenvalue-based techniques require higher computational cost, the improved sensing reliability achieved under low SNR and realistic channel conditions may justify the additional processing overhead. Since spectrum sensing in the LoRaCog architecture is performed at gateway nodes rather than at resource-constrained end devices, the additional computational burden of eigenvalue-based sensing techniques is more manageable.

The improved sensing reliability observed under low SNR and noise uncertainty conditions may help reduce channel access failures and improve spectrum utilization in dense IoT environments. However, practical implementation of SIMO-based sensing approaches may require additional RF chains, multiple antenna elements, and increased processing capabilities at the gateway level, resulting in higher hardware cost, energy consumption, and implementation complexity.

8. Conclusions

In this study, four eigenvalue-based spectrum sensing algorithms were analyzed within the LoRa cognitive framework to evaluate their performance using the conventional ED algorithm as a reference in different operating environments and to assess their suitability.

The results indicate that the ED algorithm achieves the best sensing performance under ideal AWGN channel conditions and exhibits the shortest sensing time. However, ED performance deteriorates significantly in the presence of noise uncertainty and multipath propagation effects. On the contrary, a noticeable improvement in performance was observed under the same conditions when eigenvalue-based algorithms were employed. These algorithms demonstrated higher reliability in non-ideal wireless environments because they rely on the statistical properties of the received signal rather than on accurate knowledge of the noise power.

In the final scenario, where spatial diversity was simulated through signal reception using multiple antennas, the MME detector outperformed the other algorithms investigated in terms of detection probability. These findings demonstrate the effectiveness of using the eigenvalue distribution of the covariance matrix when multiple signal observation branches are available.

Regarding computational sensing time, although eigenvalue-based algorithms require a relatively high computational effort due to covariance matrix construction and eigenvalue analysis, the required sensing time remains within approximately 1 to 3 ms, which is considered acceptable for gateway level sensing operations within the system.

References

[1] F. Hu, B. Chen, and K. Zhu, "Full Spectrum Sharing in Cognitive Radio Networks Toward 5G: A Survey", *IEEE Access*, vol. 6, pp. 15754–15776, 2018 (https://doi.org/10.1109/ACCESS.2018.2802450).

[2] Y. Arjoune and N. Kaabouch, "A Comprehensive Survey on Spectrum Sensing in Cognitive Radio Networks: Recent Advances, New Challenges, and Future Research Directions", *Sensors*, vol. 19, art. no. 126, 2019 (https://doi.org/10.3390/s19010126).

[3] M.U. Muzaffar and R. Sharqi, "A Review of Spectrum Sensing in Modern Cognitive Radio Networks", *Telecommunication Systems*, vol. 85, pp. 347–363, 2024 (https://doi.org/10.1007/s11235-023-01079-1).

[4] A. Nasser *et al.*, "Spectrum Sensing for Cognitive Radio: Recent Advances and Future Challenge", *Sensors*, vol. 21, art. no. 2408, 2021 (https://doi.org/10.3390/s21072408).

[5] T. Yucek and H. Arslan, "A Survey of Spectrum Sensing Algorithms for Cognitive Radio Applications", *IEEE Communications Surveys & Tutorials*, vol. 11, pp. 116–130, 2009 (https://doi.org/10.1109/SURV.2009.090109).

[6] Z.K. Farej and A.Y. Adel, "Review on LoRa Communication Technology, Its Issues, Challenges and Applications in Healthcare System", *European Journal of Computer Science and Information Technology*, vol. 12, pp. 1–17, 2024 (https://doi.org/10.37745/ejcsit.2013/vol12n8117).

[7] M. Centenaro, L. Vangelista, A. Zanella, and M. Zorzi, "Long-range Communications in Unlicensed Bands: The Rising Stars in the IoT and Smart City Scenarios", *IEEE Wireless Communications*, vol. 23, pp. 60–67, 2016 (https://doi.org/10.1109/MWC.2016.7721743).

[8] F. Salika *et al.*, "LoRaCog: A Protocol for Cognitive Radio-based LoRa Network", *Sensors*, vol. 22, art. no. 3885, 2022 (https://doi.org/10.3390/s22103885).

[9] M.K. Giri and S. Majumder, "Eigenvalue-based Cooperative Spectrum Sensing Using Kernel Fuzzy C-means Clustering", *Digital Signal Processing*, vol. 111, art. no. 102996, 2021 (https://doi.org/10.1016/j.dsp.2021.102996).

[10] Y. Zeng and Y.C. Liang, "Eigenvalue-based Spectrum Sensing Algorithms for Cognitive Radio", *IEEE Transactions on Communications*, vol. 57, pp. 1784–1793, 2009 (https://doi.org/10.1109/TCOMM.2009.06.070402).

[11] M. Bor, U. Roedig, T. Voigt, and J.M. Alonso, "Do LoRa Low-power Wide-area Networks Scale?", *Proc. of the 19th ACM International Conference on Modeling, Analysis and Simulation of Wireless and Mobile Systems (MSWiM)*, pp. 59–67, 2016 (https://doi.org/10.1145/2988287.2989163).

[12] A.J. Onumanyi, A.M. Abu-Mahfouz, and G.P. Hancke, "Cognitive Radio in Low Power Wide Area Network for IoT Applications: Recent Approaches, Benefits and Challenges", *IEEE Transactions on Industrial Informatics*, vol. 16, pp. 7489–7498, 2020 (https://doi.org/10.1109/TII.2019.2956507).

[13] K. Arshid *et al.*, "Energy Detection Based Spectrum Sensing Strategy for CRN", *2020 IEEE International Conference on Artificial Intelligence and Information Systems (ICAIIS)*, Dalian, China, 2020 (https://doi.org/10.1109/ICAIIS49357.2020.9752316).

[14] A.S.S. Musuvathi *et al.*, "Efficient Improvement of Energy Detection Technique in Cognitive Radio Networks Using K-nearest Neighbour (KNN) Algorithm", *EURASIP Journal on Wireless Communications and Networking*, vol. 2024, art. no. 10, 2024 (https://doi.org/10.1186/s13638-024-02338-8).

[15] K.P. Patil, A.S. Lande, and M.H. Naikwadi, "A Review on the Evolution of Eigenvalue Based Spectrum Sensing Algorithms for Cognitive Radio", *Network Protocols and Algorithms*, vol. 8, pp. 58–77, 2016 (https://doi.org/10.5296/npa.v8i2.9349).

[16] S. Samala, S. Mishra, and S.S. Singh, "Machine Learning and an Eigenvalue-based Technique to Improve Cooperative Spectrum Sensing in Generalized α-$\varkappa$-μ Fading Channel", *Journal of Communications*, vol. 19, pp. 222–228, 2024 (https://doi.org/10.12720/jcm.19.5.222-228).

Batool Jaafar Bashar, Master's Student
Department of Information and Communication Engineering
https://orcid.org/0009-0004-5529-6467
E-mail: batool.jafar.ie25@nahrainuniv.edu.iq
Al-Nahrain University, Baghdad, Iraq
https://nahrainuniv.edu.iq/en

Hikmat Abdullah, Professor
Department of Information and Communication Engineering
https://orcid.org/0000-0002-1133-2057
E-mail: hikmat.abdullah@nahrainuniv.edu.iq
Al-Nahrain University, Baghdad, Iraq
https://nahrainuniv.edu.iq/en